Automated 3-D Tracking of Centrosomes in Sequences of Confocal Image Stacks

Ryan A. Kerekes, Shaun S. Gleason, Niraj Trivedi, and David J. Solecki

***Abstract*— In order to facilitate the study of neuron migration, we propose a method for 3-D detection and tracking of centrosomes in time-lapse confocal image stacks of live neuron cells. We combine Laplacian-based blob detection, adaptive thresholding, and the extraction of scale and roundness features to find centrosome-like objects in each frame. We link these detections using the joint probabilistic data association filter (JPDAF) tracking algorithm with a Newtonian state-space model tailored to the motion characteristics of centrosomes in live neurons. We apply our algorithm to image sequences containing multiple cells, some of which had been treated with motion-inhibiting drugs. We provide qualitative results and quantitative comparisons to manual segmentation and tracking results showing that our average motion estimates agree to within 13% of those computed manually by neurobiologists.**

I. INTRODUCTION

Recent advances in fluorescence microscopy have enabled biologists to image cellular and subcelluar dynamic processes in live cells with the use of florescent protein tagging. Neuronal cell migration is one such biological process in which time-lapse 3-D imaging has played a key role. Recently, the centrosome, an organelle that plays a role in mitosis, has been shown to also act as a predictor of neuronal cell migration and possibly a coordinator of cytoskeletal dynamics in the neuron; moreover, certain drugs have been shown to inhibit centrosome motion and neuronal migration [1]. Thus, neurobiologists are interested in tracking centrosomes in a live cell and examining the motion characteristics with respect to both overall cell motion and the introduction of various drugs. Due to the slow and laborious nature of manual analysis, automated computational methods tailored to specific biological phenomena and imaging modalities are needed to address the high throughput of these imaging systems.

Automated tracking of subcellular structures in confocal imagery has been addressed in the literature [2]; however, the appearance and motion characteristics of different structures vary widely, and thus a method developed for one type of structure will not likely translate well to other structures. A particle filtering method, which decouples the traditional detection and tracking stages, has been proposed by Smal *et al.* [3] for tracking microtubules, which appear as small, elongated bright spots very different in appearance from centrosomes. This method utilizes probabilistic appearance models of the microtubules derived from the underlying physics of microscopic image formation. Rogers *et al.* [4] attempt to track subcellular particles of varying size by fitting a 2-D polynomial model to the appearance of each structure and discriminating based on the model parameters; however, because this method allows a great deal of freedom in the shape of tracked particles, we would expect it to follow many non-centrosome objects in our data.

In this paper, we propose a method for detecting and tracking centrosomes tagged with green fluorescent protein (GFP)

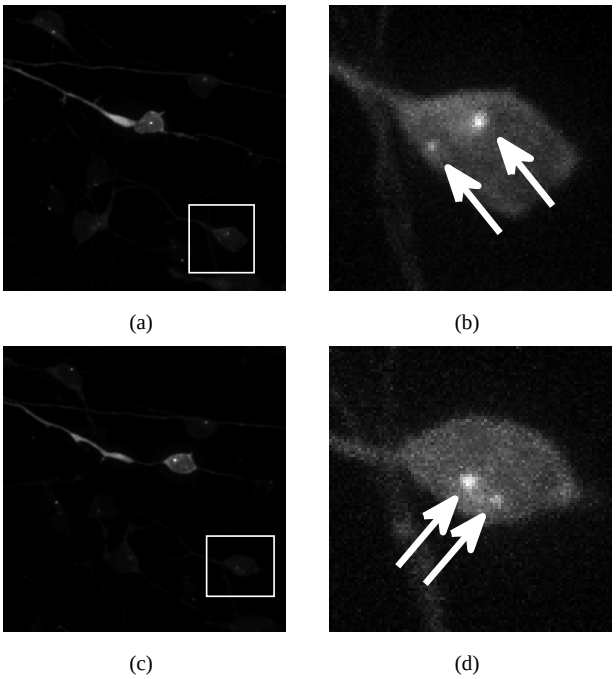

Fig. 1. Maximum intensity projections over z of a 3-D centrosome volume at two different time points: (a)-(b) $t = 0$ minutes; (c)-(d) $t = 40$ minutes. Regions of (a) and (c) delineated by boxes are enlarged in (b) and (d). Individual centrosomes are indicated with arrows. Migration of the bright cell soma in the middle of (a) and (c) can be seen by comparing its position across the two images. Note the relatively low brightness of the delineated cell in (a) and (c), whose detail can be seen when rescaled in (b) and (d). The images in (a) and (c) are approx. 80 μm in width and height.

Notice: This manuscript has been authored by UT-Battelle, LLC, under contract DE-AC05-00OR22725 with the U. S. Department of Energy. The United States Government retains and the publisher, by accepting the article for publication, acknowledges that the United States Government retains a non-exclusive, paid-up, irrevocable, world-wide license to publish or reproduce the published form of this manuscript, or allow others to do so, for United States Government purposes. Research sponsored by the Laboratory Directed Research and Development Program of Oak Ridge National Laboratory (ORNL), managed by UT-Battelle, LLC for the U. S. Department of Energy.

R. A. Kerekes and S. S. Gleason are with the Image Science and Machine Vision Group, Measurement Science and Systems Engineering Division, Oak Ridge National Laboratory, Oak Ridge, TN 37831, USA kerekesra@ornl.gov

N. Trivedi and D. J. Solecki are with the Department of Developmental Neurobiology, St. Jude Children's Research Hospital, Memphis, TN 38105

in time-lapse 3-D confocal image stacks. Our approach consists of detecting candidate centrosomes, computing discriminatory features based on the appearance characteristics of typical centrosomes to refine this set of detections, and applying a robust multi-target tracking algorithm known as the joint probabilistic data association filter (JPDAF) [5] to link the detections. We show the results of applying our algorithm to a set of time-lapse 3-D image sequences of mouse cerebellar granule cells treated with various drugs and imaged with a spinning disk confocal microscope.

II. TECHNICAL APPROACH

Our approach to automated centrosome motion analysis may be divided into two stages: (1) detection, and (2) tracking. The goal of the detection stage is to locate all centrosome-like objects in each frame of the time sequence. The tracking stage then attempts to connect these detections to form coherent tracks. The details of each stage are illustrated in Figure 1 and outlined below.

A. Centrosome detection

In the detection stage, we first compress the 3-D volume at each time step into a single 2-D image by computing a maximum intensity projection along the z-dimension. There are two reasons for working in 2-D for the detection stage: (1) computation is greatly reduced compared to 3-D, and (2) the resolution in z was significantly lower than that of x and y in our datasets, which would necessitate interpolation in z in order to compute certain features. It should be noted that we later utilize the full volume to compute 3-D centrosome positions.

We apply a Laplacian filter to this image, which helps to accentuate small, bright, circularly-shaped regions in the image [6]. We apply an adaptive threshold to the filtered image by first computing the mean μ and standard deviation σ of the intensity values in a small window of size $N_O \times N_O$ surrounding each pixel. We exclude a smaller window of size $N_I \times N_I$ around the peak in this computation in order to prevent the peak itself from contributing to the window statistics. Each pixel location whose value v is such that

$$\frac{v-\mu}{\sigma} > T \tag{1}$$

for some threshold T is declared to be a candidate centrosome location. We used $N_O = 30$ and $N_I = 12$ in our work.

We refine this set of detections by computing two additional metrics for each candidate centrosome: (1) object size and (2) local roundness. Object size is measured by computing a scale-space representation of the pattern, akin to the approach of Bretzner and Lindeberg [7]. Specifically, for each candidate centrosome, we project the pattern onto a sequence of 2-D Laplacian-of-Gaussian operators at increasing σ values. We then find the value σ_0 at which the projection is minimized (most negative). If $\sigma_0 \notin [\sigma_L, \sigma_H]$ for the scale range defined by the limits σ_L and σ_H, then the detection is discarded. In this work, we found $(\sigma_L, \sigma_H) = (1, 8)$ to work well.

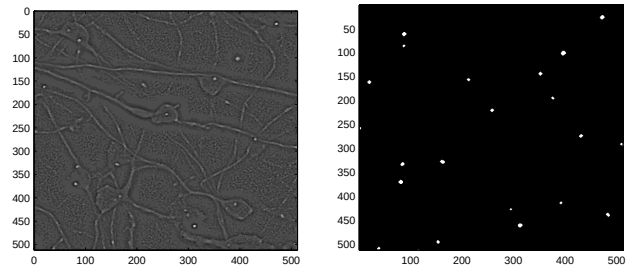

(a) (b)

Fig. 2. Example of centrosome detection: (a) adaptive threshold image just before comparing to T (Eq. 1); (b) detected candidate centrosomes using threshold equal to 10. The refined set of detection after roundness- and scale-based filtering is shown in Fig. 4(c).

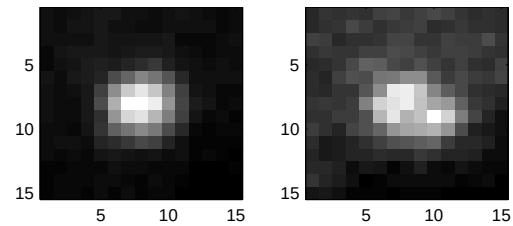

(a) $\rho = 0.98$ (b) $\rho = 0.91$

Fig. 3. Examples of roundness metrics computed for two different patterns using (3).

Because centrosomes typically appear as round sphere-like objects in our imagery, we use the local roundness of each candidate detection as a discriminative feature. Local roundness in 2-D can be defined as the constancy of a pattern along various concentric circles centered about a given point. We measure local roundness by first computing the rotational autocorrelation of the candidate centrosome pattern as follows. Let $f(r, \theta)$ denote the local 2-D pattern in polar coordinates, centered about the detection location. We define the rotational autocorrelation function $R_{ff}(\phi)$ of f by the following equation:

$$R_{ff}(\phi) = \frac{\int_0^{2\pi} \int_{r_1}^{r_2} f(r,\theta) f(r, \theta - \phi) r dr d\theta}{\int_0^{2\pi} \int_{r_1}^{r_2} f^2(r,\theta) r dr d\theta}, \tag{2}$$

where r_1 and r_2 are the inner and outer radii between which the pattern is considered. Using this function, we then compute a roundness metric ρ given by the following equation:

$$\rho = 1 - \sqrt{\frac{1}{2\pi} \int_0^{2\pi} R_{ff}(\theta) d\theta}. \tag{3}$$

The integral in (3) essentially measures the variance of $R_{ff}(\phi)$ (with an assumed mean of 1). For a perfectly "round" object, ρ would evaluate to 1, since the variance would be 0; on the other hand, for a random pattern, $R_{ff}(\phi)$ would approach a delta function and ρ would be close to zero. We compare this roundness metric to a threshold T_ρ and discard the detection if $\rho < T_\rho$. In our work, we used $T_\rho = 0.92$ and $(r_1, r_2) = (0.2, 4.0)$ pixels. Examples of roundness values are shown in Fig. 3.

For each remaining detection, we compute the z-position by first extracting the column of intensity values at the corresponding (x, y) location from the original volume. We then upsample this signal by a factor of 8 and smooth using sinc interpolation. The z-position of the centrosome is then taken to be the location where this signal reaches its maximum. It should be noted that this approach would fail to detect multiple centrosomes centered at the same (x, y) location in the volume, and a more elaborate method should be used to detect multiple centrosomes at a given (x, y) location if overlap in z is suspected.

B. Centrosome tracking

Once we have the detections for each frame, we then take the following approach to tracking the objects. Based on the assumption that no centrosome will jump by more than a predefined distance d between any two consecutive frames, we first partition the set of all detections over the entire sequence such that the Euclidean distance between any two detections from different groups is greater than d. We then apply the well-known JPDAF tracking algorithm [5] to each group of detections, which is designed to handle multiple targets, missed detections, false alarms, and measurement noise.

The JPDAF algorithm requires a user-defined state-space model that describes the motion of the objects to be tracked. In our time-lapse sequences, we observed that the motion of centrosomes seems to be characterized by bursts of acceleration in (seemingly) random directions. We therefore employed a Newtonian 3-D motion model that provides for random acceleration in x, y, and z characterized by independent Gaussian random variables. The state update and observation equations for our model are as follows. Let $\mathbf{x}$ denote the state vector

$$\mathbf{x} = [\ x\ y\ z\ \dot{x}\ \dot{y}\ \dot{z}\ ]^{\mathrm{T}}, \tag{4}$$

where $\dot{x}$, $\dot{y}$, and $\dot{z}$ are the velocities in the respective directions. Then the state $\mathbf{x}_k$ at time k is updated as

$$\mathbf{x}_k = \mathbf{F}\mathbf{x}_{k-1} + \mathbf{G}\mathbf{w}_k \tag{5}$$

where

$$\mathbf{w}_k \sim \mathcal{N}(0, \mathbf{I}_3), \tag{6}$$

$$\mathbf{F} = \begin{bmatrix} \mathbf{I}_3 & \Delta t \cdot \mathbf{I}_3 \\ \mathbf{0}_3 & \mathbf{I}_3 \end{bmatrix}, \tag{7}$$

and

$$\mathbf{G} = \sigma_a \begin{bmatrix} \frac{\Delta t^2}{2} \cdot \mathbf{I}_3 \\ \Delta t \cdot \mathbf{I}_3 \end{bmatrix} + \sigma_n \begin{bmatrix} \mathbf{I}_3 \\ \mathbf{0}_3 \end{bmatrix} \tag{8}$$

where $\mathbf{I}_3$ is the 3×3 identity matrix and $\mathbf{0}_3$ is the 3×3 matrix of zeros. In (8), σ_a^2 and σ_n^2 are the variances of the random acceleration and an additional position "noise" factor, respectively, undergone by each centrosome in the x, y, and z directions. Strictly speaking, a random acceleration model alone (supplied by the σ_a term) should allow for any change in centrosome position; nevertheless, including the σ_n term instinctively provides a better model for describing small "vibrating" motions observed in many of the centrosomes.

The observation $\mathbf{z}_k = [\ x'\ y'\ z'\ ]$ our state-space model is given by

$$\mathbf{z}_k = \mathbf{H}\mathbf{x}_k + \mathbf{v}_k \tag{9}$$

where

$$\mathbf{v}_k \sim \mathcal{N}(0, \sigma_m^2 \mathbf{I}_3), \tag{10}$$

and

$$\mathbf{H} = \begin{bmatrix} 1 & 0 & 0 & 0 & 0 & 0 \\ 0 & 1 & 0 & 0 & 0 & 0 \\ 0 & 0 & 1 & 0 & 0 & 0 \end{bmatrix}. \tag{11}$$

The variables x', y', and z' are the observed 3-D coordinates of the centrosome, and σ_m^2 is the variance of the measurement noise resulting from small errors in locating the center of the centrosome.

We initialize the tracker with starting locations by selecting the N (at most) brightest objects from each group of detections in the first frame of the sequence (we found $N = 6$ to work well). For each target at each time instant, the JPDAF algorithm computes the probability of missed detection, indicating the likelihood of having failed to detect the target in the current frame. In our implementation, we retire a track if this probability is greater than 0.5 for four consecutive frames. In future work, the initialization stage may be improved by utilizing more than just the first frame in case a detection was missed in that frame.

III. DATA

Image data was collected from nine separate experiments, where each experiment was designed to capture time-lapse 3-D imagery of a culture of cerebellar granule neurons (CGNs) over the course of several hours. The CGNs were cultured in conditions that supported cellular motility, and an expression vector was introduced to the CGNs to encode the centrosomes. At specified times during the experiment, a sequence of 3-D volumes of size $512 \times 512 \times 15$ voxels was imaged using a Marianas spinning disk confocal microscope. The resolution of the volume was 0.157 μm/pixel in x and y and 1 μm/pixel in z, resulting in an imaged volume of size $80 \times 80 \times 15$ μm.

Sequences of 20 3-D frames were acquired at a rate of one frame per 16 seconds, and such sequences were captured at times $t < 0$, $t = 10$ min, $t = 40$ min, and $t = 60$ min, where a treatment was (in some cases) introduced to the cells at time $t = 0$. Two different treatments were used in these experiments: Jasplakinolide, a cell permeable actin stabilizer, and Blebbistatin, a cell permeable Myosin II inhibitor. These drugs were used to study the role of the actin cytoskeleton in centrosome and somal motility. Each of these drugs was used in three of the experiments. In order to create a control set, three additional experiments were conducted in which no drug was introduced.

IV. RESULTS

We applied our algorithm to sequences from the nine experiments described above. In order to illustrate the output of our algorithm, we first show examples of computed centrosome tracks for a 20-frame sequence prior to being

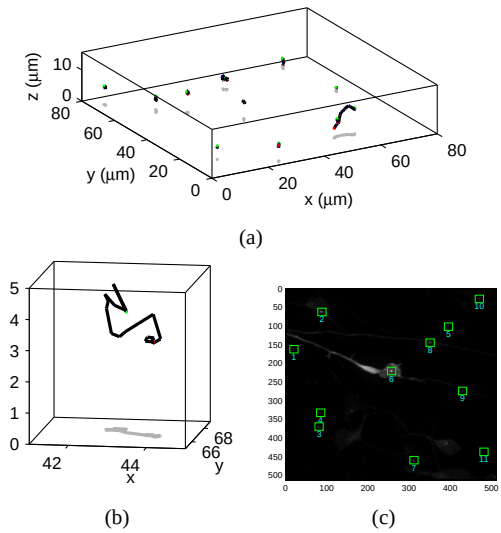

Fig. 4. Centrosome tracks from a single sequence: (a) whole volume in 3-D; (b) zoomed view of a single track in 3-D; (c) track starting points projected onto x-y plane and superimposed on first frame of sequence. Shadows are shown on the x-y plane for shape emphasis.

TABLE I

TOTAL NUMBER OF CENTROSOMES TRACKED

	Treatment		
	Blebbistatin	Jasplakinolide	control set
Proposed algorithm	552	318	395
Manual segmentation	559	471	542

treated with Blebbistatin. 3-D centrosome tracks within the volume are shown in Figs. 4(a) and 4(b). In Fig. 4(c), we show the initial centrosome positions in the x-y plane superimposed onto the maximum intensity projection (over z) of the first frame of the sequence.

We compared the results of our algorithm with those generated from manual segmentation and tracking of the centrosomes by neurobiologists. Because manual data about individual centrosome positions was not available, we were only able to compare aggregate velocity measurements. There are two main factors that account for discrepancies between the results: (1) the manual measurements were performed on 2-D projection images rather than the 3-D volumes themselves, thus ignoring one dimension of motion; (2) the manual segmentation discarded centrosomes that were not contained within the soma. Table I shows the total number of centrosomes tracked over all sequences for each treatment. Our algorithm tended to reject many low-contrast centrosomes that were identified in the manual segmentation, resulting in fewer tracked centrosomes on average. We computed average velocity and peak velocity averaged over all centrosomes at each time step for the different treatment types, shown in Fig. 5 for comparison.

V. CONCLUSIONS AND FUTURE WORK

We proposed a new algorithm for detecting and tracking centrosomes in 3-D time-lapse imagery. Although we tracked fewer centrosomes than were tracked manually, we were able

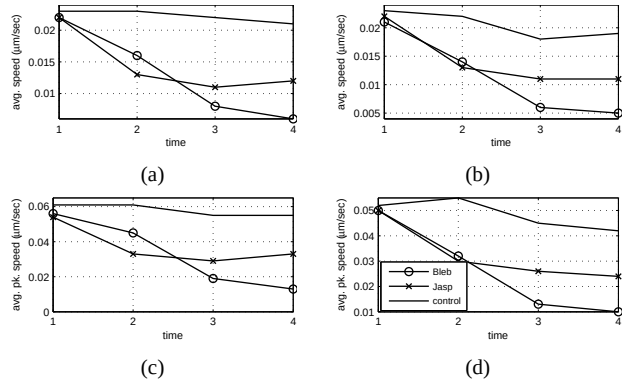

Fig. 5. Plots of centrosome average speed and peak speed averaged over all centrosomes in each treatment type: versus experiment time: (a), (c) results produced by the new algorithm; (b), (d) manual results. Times on the x-axis are denoted by 1 ($t < 0$), 2 ($t = 10$ min), 3 ($t = 40$ min), and 4 ($t = 60$ min).

to sample and track the population such that our aggregate motion metrics agree with manually generated aggregate results to within 13% for average centrosome speed and to within 34% for peak centrosome speed. In these studies, such metrics are of greater importance from an experimental standpoint than the individual tracks themselves. Thus, we believe that our proposed algorithm would be useful to neurobiologists in analyzing the large volumes of data necessary for advancing the study of neuronal migration.

In order to more fully study cell migration from a biological perspective, it is necessary to examine not only centrosome motion but also the motion of the cell bodies themselves. In this work, we focused only on centrosome motion; thus, it will be of interest in future work to perform automatic segmentation and tracking of cell somas in the same time-lapse imagery. Furthermore, centrosome motion should be correlated with the motion of their respective soma in order to make observations about predictive behavior and develop biological models.

REFERENCES

[1] D. J. Solecki, L. Model, J. Gaetz, T. M. Kapoor, and M. E. Hatten, "Par6α signaling controls glial-guided neuronal migration," *Nature Neuroscience*, vol. 7, pp. 1195–1203, Nov. 2004.

[2] E. Meijering, I. Smal, and G. Danuser, "Tracking in molecular bioimaging," *IEEE Signal Processing Mag.*, pp. 46–53, May 2006.

[3] I. Smal, K. Draegestein, N. Galjart, W. Niessen, and E. Meijering, "Particle filtering for multiple object tracking in dynamic flourescence microscopy images: application to microtubule growth analysis," *IEEE Trans. Med. Imag.*, vol. 27, pp. 789–804, June 2008.

[4] S. S. Rogers, T. A. Waigh, X. Zhao, and J. R. Lu, "Precise particle tracking against a complicated background: polynomial fitting with gaussian weight," *Phys. Biol.*, vol. 4, pp. 220–227, 2007.

[5] Y. Bar-Shalom and T. E. Fortmann, *Tracking and Data Association*. New York, NY: Academic, 1988.

[6] T. Lindeberg, "Detecting salient blob-like image structures and their scales with a scale-space primal sketch: a method for focus-of-attention," *International Journal of Computer Vision*, vol. 11, pp. 283–318, 1993.

[7] L. Bretzner and T. Lindeberg, "Feature tracking with automatic selection of spatial scales," *Computer Vision and Image Understanding*, vol. 71, pp. 385–392, 1998.